Clinical and Translational Radiation Oncology 43 (2023) 100683

Contents lists available at ScienceDirect

Clinical and Translational Radiation Oncology

journal homepage: www.sciencedirect.com/journal/clinical-and-translational-radiation-oncology

Original Research Article

Symptomatic radiation-induced rib fractures after stereotactic body radiotherapy for early-stage non-small cell lung cancer

Nozomi Kita [a], Natsuo Tomita [a,*], Taiki Takaoka [a], Akane Matsuura [a], Dai Okazaki [a], Masanari Niwa [a], Akira Torii [a], Seiya Takano [a], Yuji Mekata [a], Akio Niimi [b], Akio Hiwatashi [a]

[a] Department of Radiology, Nagoya City University Graduate School of Medical Sciences, 1 Kawasumi, Mizuho-cho, Mizuho-ku, Nagoya, Aichi 467-8601, Japan
[b] Department of Respiratory Medicine, Allergy and Clinical Immunology, Nagoya City University Graduate School of Medical Sciences, 1 Kawasumi, Mizuho-cho, Mizuho-ku, Nagoya, Aichi 467-8601, Japan

ARTICLE INFO

Keywords:
Stereotactic body radiation therapy
Non-small cell lung cancer
Rib fracture
Toxicity

ABSTRACT

Background and purpose: The present study investigated the relationships between the risk of radiation-induced rib fractures (RIRF) and clinical and dosimetric factors in stereotactic body radiotherapy (SBRT) for early-stage non-small cell lung cancer (NSCLC). We also examined dosimetric parameters associated with symptomatic or asymptomatic RIRF and the dosimetric threshold for symptomatic RIRF.
Materials and methods: We reviewed 244 cases of early-stage NSCLC treated with SBRT. Gray's test and the Fine-Gray model were performed to examine the relationships between clinical and dosimetric factors and grade $\geq$ 2 (i.e., symptomatic) RIRF. The effects of each dose parameter on grade $\geq$ 1 and $\geq$ 2 RIRF were assessed with the Fine-Gray model. The *t*-test was used to compare each dose parameter between the grade 1 and grade $\geq$ 2 groups. Optimal thresholds were tested using receiver operating characteristic (ROC) curves.
Results: With a median follow-up period of 48 months, the 4-year cumulative incidence of grade $\geq$ 1 and grade $\geq$ 2 RIRF were 26.4 % and 8.0 %, respectively. Regarding clinical factors, only age was associated with the development of grade $\geq$ 2 RIRF ($p = 0.024$). Among dosimetric parameters, only V40Gy significantly differed between the grade 1 and grade $\geq$ 2 groups ($p = 0.015$). The ROC curve analysis of grade $\geq$ 2 RIRF showed that the optimal diagnostic thresholds for D3cc, D4cc, D5cc, and V40Gy were 45.86 Gy (area under the curve [AUC], 0.706), 39.02 Gy (AUC, 0.705), 41.62 Gy (AUC, 0.702), and 3.83 cc (AUC, 0.730), respectively. These results showed that V40Gy $\leq$ 3.83 cc was the best indicator of grade $\geq$ 2 RIRF. The 4-year incidence of grade $\geq$ 2 RIRF in the V40Gy $\leq$ 3.83 cc vs. $>$ 3.83 cc groups was 1.8 % vs. 14.2 % ($p = 0.001$).
Conclusion: The present results recommend V40Gy $\leq$ 3.83 cc as the threshold for grade $\geq$ 2 RIRF in SBRT.

Introduction

Stereotactic body radiotherapy (SBRT) is a standard treatment option for patients with medically inoperable early-stage non-small cell lung cancer (NSCLC), offering the potential for better tumor control and longer overall survival. Recent findings highlighted SBRT as a treatment option for operable early-stage NSCLC and oligometastatic lung tumors, further emphasizing its importance [1–5].

While SBRT is generally a safe treatment for early-stage NSCLC, it is associated with some toxicities, such as radiation-induced rib fractures (RIRF). The reported incidence of symptomatic and asymptomatic RIRF typically ranges between approximately 5 and 30 % [6–9]. The course of RIRF varies from mild cases to those accompanied by severe pain. Painful RIRF is clinically important because of its impact on quality of life. Clinical risk factors for and optimal dosimetric parameters to mitigate the risk of symptomatic RIRF in patients undergoing SBRT currently remain unclear. Therefore, the present study investigated the relationships between the risk of RIRF and clinical and dosimetric factors in SBRT for early-stage NSCLC. We also examined dosimetric parameters associated with symptomatic or asymptomatic RIRF and the dosimetric threshold for symptomatic RIRF.

* Corresponding author.
E-mail address: c051728@yahoo.co.jp (N. Tomita).

https://doi.org/10.1016/j.ctro.2023.100683
Received 29 August 2023; Accepted 21 September 2023
Available online 25 September 2023

Materials and Methods

Study population

The present study analyzed the medical documents of early-stage NSCLC patients who underwent SBRT at our institution between February 2004 and September 2018. In accordance with ethical protocols, informed consent was acquired from each patient prior to commencing treatment. Inclusion criteria encompassed: 1) patients clinically classified as Tis-T2bN0M0 according to the 8th TNM classification; 2) treatment with SBRT; 3) patients histologically diagnosed with NSCLC or strongly presumed to be NSCLC based on diagnostic imaging results and the trajectory of their clinical progression. Among 245 patients who satisfied these prerequisites, one was omitted from the final analysis due to an inability to precisely assess their dose-volume histogram (DVH) data. Therefore, 244 cases were included in the final study cohort. The Institutional Review Board of Nagoya City University Graduate School of Medical Sciences approved this research (approval number: 60–22-0024), ensuring it adhered to the ethical parameters outlined in the 1964 Declaration of Helsinki and its subsequent amendments. Due to the retrospective nature of the present study, the necessity for written informed consent was waived and an opt-out form was accessible on the website for those opting against participation.

Pretreatment evaluation

Clinical staging was conducted based on the findings of chest and upper abdomen computed tomography (CT), magnetic resonance imaging (MRI) or CT of the brain, and 18F-fluoro-deoxyglucose positron emission tomography (FDG-PET). Bone scintigraphy was utilized when FDG-PET was not accessible. The applicability of SBRT for each case was evaluated through a collaborative consultation at a multidisciplinary tumor board.

SBRT methods

SBRT planning procedures were documented in previous studies [10–12]. A triphasic CT scan, encompassing normal breathing, the expiratory phase, and inspiratory phase, was performed with a slice thickness of 2.5 mm. The gross tumor volume (GTV) was delineated based on CT and/or FDG-PET findings. The clinical target volume (CTV) was established as equal to GTV, with fluoroscopy employed to gauge the tumor's respiratory movement. To cover CTV in all respiratory phases, an internal target volume (ITV) was generated, with supplementary anisotropic margins of 5 mm in the lateral and anteroposterior directions, and 5–10 mm in the craniocaudal direction added to ITV to formulate PTV. Metallic markers were utilized during irradiation for patients showing significant respiratory motion while breath-hold was maintained. The necessity for this technique was ascertained when displacement visible in fluoroscopy was $\geq$ 1 cm. Metallic markers were Visicoil or Gold Anchor. We predominantly relied on expiration CT scans for contouring. PTV was formulated by extending a 6-mm margin from GTV in all directions. This breath-hold technique was employed for 8 patients.

Dosages, using a 6 MV photon beam directed at the PTV's isocenter, were selected by the tumor diameter. By taking radiobiological factors into consideration, SBRT was conducted twice weekly in four fractions, ensuring a minimum three-day gap between each treatment session [13]. Each treatment was generally scheduled at least 72 h apart; however, due to constraints regarding patient and machine availability, the actual median treatment duration was 12 days. A minimum of 90 % of the isocenter dose was suggested to cover 95 % of PTV. There were no specific guidelines concerning minimum and maximum doses. Nevertheless, in most SBRT plans, the minimum and maximum doses for PTV were higher than 80 % and lower than 107 % of the prescription doses, respectively. Prior to November 2008, prescribed doses of 44, 48, and 52 Gy were allocated for peripheral tumors with maximum diameters $<$ 1.5 cm, 1.5–3 cm, and $>$ 3 cm, respectively. The protocol for dose escalations was amended from December 2008, and planned doses of 48, 50, and 52 Gy were administered based on the respective tumor diameters. Individualized doses of 60 or 64 Gy in eight fractions were implemented for cases with proximity to the pulmonary hilum or crucial organs [14]. Between February 2004 and November 2008, pencil beam convolution with the Batho power law was utilized for dose calculations. The analytical anisotropic algorithm was employed between December 2008 and May 2015 and the collapsed cone convolution from June 2015.

Follow-up and evaluation of RIRF

Subsequent to SBRT, patients underwent CT every 2 to 3 months for up to 6 months. After this period, CT was conducted at a minimum semi-annually, with FDG-PET and brain MRI or CT being performed as necessary. The primary endpoint was established as the development of grade $\geq$ 2 RIRF. RIRF was diagnosed by employing a combination of CT scans and clinical symptomatology. The gradation of RIRF was classified in alignment with the Common Terminology Criteria for Adverse Events version 5.0: grade 1 is asymptomatic and clinical or diagnostic observations only, grade 2 is symptomatic and requires analgesics, grade 3 is severe symptoms and operative intervention indicated, grade 4 is life-threatening consequences and urgent intervention indicated, and grade 5 is death.

Dose-volume analyses

DVH data and dose distribution information were meticulously analyzed using RayStation software (RaySearch Medical Laboratories AB, Stockholm, Sweden). Most cases underwent SBRT in 4 fractions. Among patients who received treatment in 6 or 8 fractions, DVH data were converted to a 4-fraction equivalent using an α/β value of 3. Vn represents the volume of the rib receiving a minimum dose of n Gy. Dx cc is a dosimetric metric that signifies the dose absorbed by the most exposed $\times$ cubic centimeters of the rib. Parameters including Dmax, D0.5cc, D1cc, D2cc, D3cc, D4cc, D5cc, V20, V25, V30, V40, and V50 were deduced from DVH.

Statistical analysis

Gray's test was employed to examine the relationships between risk factors and grade $\geq$ 2 RIRF, implementing the Fine-Gray model in a multivariable analysis, accounting for mortality as a competing risk. The effect of each dose parameter on RIRF was assessed using the Fine-Gray model, while death remained as a competing risk. The comparison of dosimetric factors between the group with only grade 1 RIRF and the group with grade $\geq$ 2 RIRF was conducted using the *t*-test. Optimal thresholds for every dose parameter were selected using receiver operating characteristic (ROC) curves. The significance of differences was set at a p-value $<$ 0.05. Statistical analyses were performed using EZR (Saitama Medical Center, Jichi Medical University, Saitama, Japan), which is a graphical user interface for R (The R Foundation for Statistical Computing, Vienna, Austria) [15].

Results

A total of 244 patients were included, with a median follow-up period of 48 months (range, 0–198) for all patients, and 59 months (range, 0–198) for living patients. Table 1 shows patient characteristics and treatment specifics. The patient cohort had a median age of 77 years. Grade $\geq$ 1 RIRF were observed in 57 cases (23.4 %), of which 20 (8.2 %) were classified as grade $\geq$ 2 RIRF. No grade 3 or higher RIRF was observed. Among cases with RIRF, the percentage of symptomatic (i.e., grade $\geq$ 2) patients was 35.1 %. The median times to the onset of grade

Table 1
Patient and treatment characteristics.

Characteristics	Number or median	% or range
Age (years)	77	29–89
Sex		
Male	169	69 %
Female	75	31 %
PS		
0	117	48 %
1	101	41 %
2	23	9 %
Missing	3	1 %
Smoker		
Current	70	29 %
Ex	107	44 %
Non	60	25 %
Missing	7	3 %
Solid component diameter (mm)	23	0–50
Total dose (Gy)	50	44–64
Fractions	4	4–8
BED10	112.5	92.4–120

PS, performance status; BED10, biologically effective dose calculated with an α/β value of 10.

≥ 1 and grade ≥ 2 RIRF were 20 months (range, 5–160) and 18 months (range, 5–86), respectively. The 4-year cumulative incidence of grade ≥ 1 and grade ≥ 2 RIRF were 26.4 % (95 % confidence interval [CI], 20.4–32.7) and 8.0 % (95 % CI, 4.9–12.0), respectively (Fig. 1).

Table 2 shows differences in the 4-year incidence of grade ≥ 2 RIRF with each clinical and dosimetric risk factor. Due to correlations among dosimetric factors, only the maximum dose (Dmax) of the rib was analyzed. Only age correlated with the development of grade ≥ 2 RIRF (p = 0.028). Table 3 shows the results of the multivariate analysis, in which the relationships between risk factors and grade ≥ 2 RIRF were examined. In the multivariate analysis, age (hazard ratio [HR] 0.28, 95 % CI 0.10–0.85, p = 0.024) and Dmax (HR 2.73, 95 % CI 1.05–7.10, p = 0.039) remained significant factors for grade ≥ 2 RIRF.

Table 4 shows the results of the univariate analysis of dosimetric

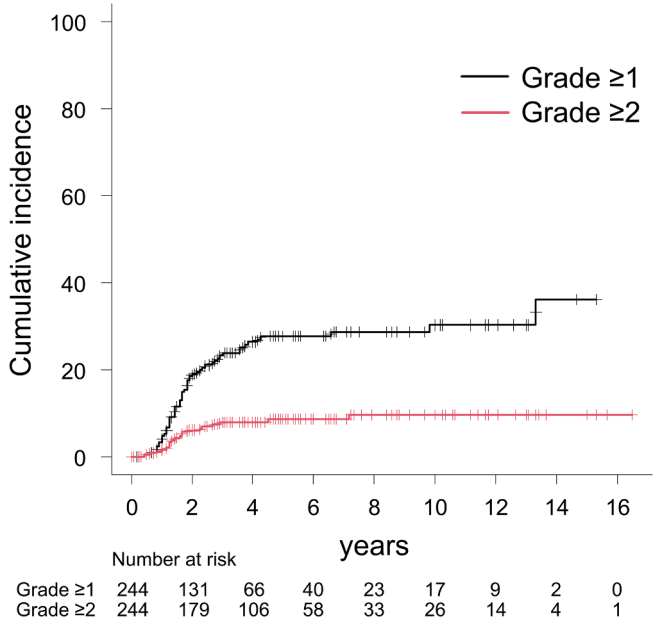

Fig. 1. Differences in the cumulative incidence of grade ≥ 1 and grade ≥ 2 radiation-induced rib fractures.

Table 2
Differences in the cumulative incidence of grade ≥ 2 radiation-induced rib fractures according to clinical and dosimetric factors.

Characteristics	Number	4-year incidence	95 % CI	*p*-value
Age (years)				0.028
≤77	134	11.1 %	6.4–17.3	
>77	110	4.2 %	1.3–9.6	
Sex				0.19
Male	169	5.8 %	2.8–10.3	
Female	75	12.8 %	6.2–21.8	
PS				0.59
0, 1	218	8.3 %	5.0–12.6	
2, 3	26	4.6 %	0.3–19.8	
Smoker				0.70
Yes	177	7.5 %	4.1–12.3	
No	60	10.3 %	4.2–19.8	
Solid component diameter (mm)				0.42
≤23	126	8.5 %	4.3–14.4	
>23	118	7.4 %	3.5–13.4	
Rib Dmax (Gy)				0.12
≤49.46	122	4.4 %	1.6–9.4	
>49.46	122	11.7 %	6.5–18.5	

95 % CI, 95 % confidence interval; PS, performance status.

Table 3
Multivariate analysis of clinical and dosimetric factors for grade ≥ 2 radiation-induced rib fractures.

Factors	HR	95 % CI	*p*-value
Age (>77 vs. ≤ 77 years)	0.28	0.10–0.85	0.024
Sex (male vs. female)	0.47	0.14–1.56	0.22
PS (2, 3 vs. 0, 1)	0.60	0.06–5.71	0.66
Smoker	1.31	0.41–4.17	0.64
Solid component diameter (mm) (>23 vs ≤ 23)	0.70	0.26–1.88	0.48
Rib Dmax (Gy) (>49.46 vs. ≤ 49.46)	2.73	1.05–7.10	0.039

HR, hazard ratio; 95 % CI, 95 % confidence interval; PS, performance status.

Table 4
Dosimetric analysis of grade ≥ 1 and grade ≥ 2 radiation-induced rib fractures.

Factors	Grade ≥ 1 rib fractures			Grade ≥ 2 rib fractures		
	HR	95 %CI	p-value	HR	95 %CI	p-value
Rib Dmax (Gy)	1.08	1.06–1.11	<0.001	1.07	1.03–1.11	<0.001
Rib D0.5 cc (Gy)	1.11	1.08–1.13	<0.001	1.09	1.05–1.14	<0.001
Rib D1cc (Gy)	1.11	1.08–1.14	<0.001	1.11	1.05–1.17	<0.001
Rib D2cc (Gy)	1.09	1.05–1.12	<0.001	1.11	1.05–1.18	<0.001
Rib D3cc (Gy)	1.07	1.04–1.10	<0.001	1.11	1.05–1.16	<0.001
Rib D4cc (Gy)	1.06	1.03–1.08	<0.001	1.09	1.04–1.14	<0.001
Rib D5cc (Gy)	1.05	1.02–1.07	<0.001	1.07	1.03–1.12	0.001
Rib V50Gy (cc)	1.04	0.96–1.12	0.32	1.10	1.03–1.18	0.005
Rib V40Gy (cc)	1.05	1.02–1.09	0.001	1.10	1.07–1.14	<0.001
Rib V30Gy (cc)	1.04	1.01–1.06	0.003	1.07	1.04–1.11	<0.001
Rib V25Gy (cc)	1.03	1.01–1.05	0.005	1.05	1.02–1.09	0.001
Rib V20Gy (cc)	1.02	1.00–1.04	0.020	1.04	1.01–1.07	0.010

HR, hazard ratio; 95 % CI, 95 % confidence interval; Vn, volume of the rib receiving a minimum dose of n Gy; Dx cc, dose absorbed by the most exposed × cubic centimeters of the rib.

Table 5
Comparison of dose parameters between grade 1 and grade ≥ 2 radiation-induced rib fractures.

Factors	Grade 1 rib fractures		Grade ≥ 2 rib fractures		*p*-value
	Mean	SD	Mean	SD	
Rib Dmax (Gy)	51.70	5.54	50.92	3.09	0.56
Rib D0.5 cc (Gy)	50.19	4.59	49.75	3.27	0.71
Rib D1cc (Gy)	49.10	4.05	49.16	3.47	0.96
Rib D2cc (Gy)	46.69	5.75	47.98	4.05	0.38
Rib D3cc (Gy)	44.06	7.14	46.67	4.91	0.15
Rib D4cc (Gy)	41.47	8.14	44.84	5.99	0.11
Rib D5cc (Gy)	38.89	8.50	42.39	8.03	0.14
Rib V50Gy (cc)	1.04	1.73	2.44	5.78	0.18
Rib V40Gy (cc)	5.55	2.57	8.89	7.37	0.015
Rib V30Gy (cc)	9.33	3.90	12.84	9.29	0.050
Rib V25Gy (cc)	12.19	5.11	15.57	10.44	0.11
Rib V20Gy (cc)	16.45	6.85	19.99	11.77	0.16

SD, standard deviation; Vn, volume of the rib receiving a minimum dose of n Gy; Dx cc, dose absorbed by the most exposed × cubic centimeters of the rib.

factors. All dosimetric factors, except for V50Gy, correlated with grade ≥ 1 RIRF, while all correlated with grade ≥ 2 RIRF. Table 5 shows comparisons of each dose parameter between the grade 1 and grade ≥ 2 groups. Only V40Gy was significantly higher in the grade ≥ 2 group than in the grade 1 group (p = 0.015).

The optimal threshold for dosimetric factors related to grade ≥ 2 RIRF was evaluated using a ROC curve analysis, and Table 6 shows the results obtained. Fig. 2 shows the ROC curves of dosimetric factors that had an AUC > 0.70. The ROC curve analysis revealed that the optimal diagnostic thresholds for D3cc, D4cc, D5cc, and V40Gy were 45.86 Gy (area under the curve [AUC], 0.706), 39.02 Gy (AUC, 0.705), 41.62 Gy (AUC, 0.702), and 3.83 cc (AUC, 0.730), respectively. The 4-year cumulative incidence of grade ≥ 2 RIRF was compared between values above and below the ROC threshold using Gray's test. The results obtained are summarized in Table 7. The results of the *t*-test, ROC curve analysis, and Gray's test showed that V40Gy ≤ 3.83 cc was the best indicator of grade ≥ 2 RIRF among the dose parameters tested. The 4-year incidence of grade ≥ 2 RIRF in the V40Gy ≤ 3.83 cc vs. > 3.83 cc groups was 1.8 % vs. 14.2 % (p = 0.001).

Discussion

We examined the incidence of RIRF in 244 patients with early-stage NSCLC treated with SBRT and analyzed risk factors for RIRF. The results obtained showed that the 4-year cumulative incidence of RIRF was 26.4 %, while that of grade ≥ 2 RIRF was 8.0 %. The percentage of symptomatic patients was 35.1 %. The reported incidence of RIRF has been reported to vary between approximately 5 and 30 % [6–9]. In the

Table 6
Dose threshold and area under the curve for grade ≥ 2 radiation-induced rib fractures.

Factors	Threshold	AUC	95 % CI
Rib Dmax (Gy)	48.20	0.627	0.519–0.736
Rib D0.5 cc (Gy)	47.80	0.656	0.554–0.758
Rib D1cc (Gy)	47.05	0.665	0.567–0.762
Rib D2cc (Gy)	47.11	0.690	0.596–0.783
Rib D3cc (Gy)	45.86	0.706	0.617–0.795
Rib D4cc (Gy)	39.02	0.705	0.614–0.796
Rib D5cc (Gy)	41.62	0.702	0.603–0.801
Rib V50Gy (cc)	0.11	0.593	0.469–0.717
Rib V40Gy (cc)	3.83	0.730	0.640–0.821
Rib V30Gy (cc)	3.91	0.692	0.595–0.790
Rib V25Gy (cc)	8.18	0.672	0.572–0.772
Rib V20Gy (cc)	13.56	0.650	0.543–0.758

AUC, area under the curve; 95 % CI, 95 % confidence interval; Vn, volume of the rib receiving a minimum dose of n Gy; Dx cc, dose absorbed by the most exposed × cubic centimeters of the rib.

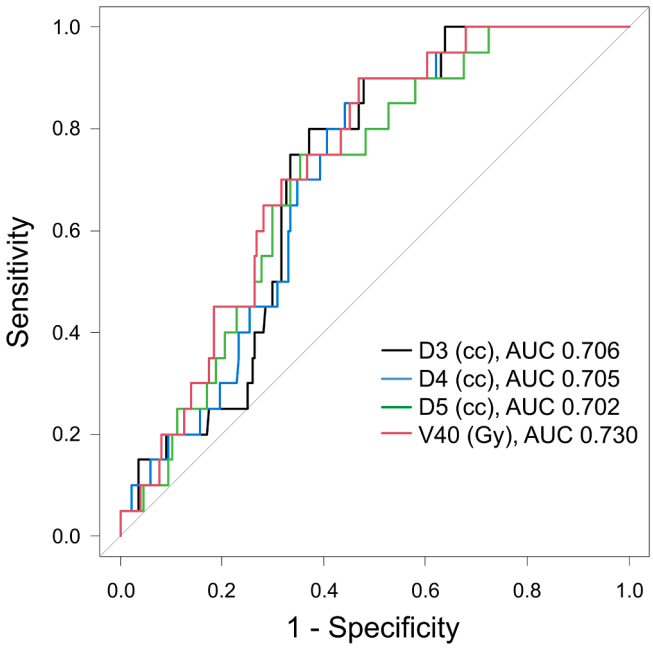

Fig. 2. Receiver operating characteristic (ROC) curves for predicting grade ≥ 2 radiation-induced rib fractures using D3, D4, D5, and V40.

Table 7
Differences in the cumulative incidence of grade ≥ 2 radiation-induced rib fractures according to each dosimetric threshold.

Factors	Number	4-year incidence	95 % CI	*p*-value
Rib Dmax (Gy)				
≤48.2	79	2.6 %	0.5–8.2	0.084
>48.2	165	10.6 %	6.3–16.1	
Rib D0.5 cc (Gy)				
≤47.8	117	2.8 %	0.7–7.3	0.026
>47.8	127	12.9 %	7.5–19.7	
Rib D1cc (Gy)				
≤47.05	113	1.8 %	0.4–5.9	0.012
>47.05	131	13.4 %	8.0–20.2	
Rib D2cc (Gy)				
≤47.11	147	3.0 %	1.0–7.0	0.003
>47.11	97	15.5 %	8.9–23.7	
Rib D3cc (Gy)				
≤45.86	146	2.2 %	0.6–5.9	<0.001
>45.86	98	16.5 %	9.7–24.8	
Rib D4cc (Gy)				
≤39.02	122	1.8 %	0.3–5.8	0.001
>39.02	122	14.2 %	8.5–21.3	
Rib D5cc (Gy)				
≤41.62	151	3.6 %	1.3–7.6	0.003
>41.62	93	15.0 %	8.4–23.4	
Rib V50Gy (cc)				
≤0.11	151	5.1 %	2.2–9.7	0.068
>0.11	93	12.8 %	6.8–20.9	
Rib V40Gy (cc)				
≤3.83	122	1.8 %	0.3–5.8	0.001
>3.83	122	14.2 %	8.5–21.3	
Rib V30Gy (cc)				
≤3.91	77	1.5 %	0.1–7.1	0.008
>3.91	167	11.0 %	6.7–16.5	
Rib V25Gy (cc)				
≤8.18	102	2.1 %	0.4–6.8	0.013
>8.18	142	12.2 %	7.3–18.5	
Rib V20Gy (cc)				
≤13.56	123	3.6 %	1.2–8.3	0.021
>13.56	121	12.4 %	7.1–19.2	

95 % CI, 95 % confidence interval; Vn, volume of the rib receiving a minimum dose of n Gy; Dx cc, dose absorbed by the most exposed × cubic centimeters of the rib.

present study, the incidence of RIRF was similar to previously reported values, with a 4-year cumulative incidence of 26.4 %. The median time to the onset of RIRF in the present study was 20 months, which is consistent with the pooled analysis of 57 studies [16]. Therefore, the observation period of 48 months in the present study was sufficient. SBRT is effective not only for the treatment of early-stage NSCLC, but also the management of oligometastatic lung tumors [3,5]. Since the utility of SBRT is expected to increase in the future, the management of adverse events, including RIRF, will become even more critical.

V40Gy was significantly higher in the grade $\geq$ 2 RIRF group than in the grade 1 RIRF group ($p = 0.015$). The ROC curve analysis showed that the optimal diagnostic threshold for V40Gy in relation to grade $\geq$ 2 RIRF was 3.83 cc (AUC, 0.730). Therefore, a threshold of V40Gy $\leq$ 3.83 cc is recommended for symptomatic RIRF. Limited information is currently available on the threshold for symptomatic RIRF. Previous studies suggested that dosimetric parameters of the rib, such as D0.5 cc and D2cc, correlated with RIRF [8,17]. Additionally, Dmax was identified as the most significant predictive factor for RIRF [7]. Some studies on chest wall pain indicated that V30 $\leq$ 30 cc was appropriate as a threshold [18–20]. Mutter et al. reported a correlation between V30 of the chest wall $\geq$ 70 cc and grade $\geq$ 2 chest wall pain. Regarding RIRF, high-dose regions appeared to be important predictive factors. However, dose ranges, such as 30–40 Gy, may become significant for symptomatic RIRF. In the present study, comparisons of dosimetric factors between asymptomatic and symptomatic RIRF revealed a significant difference for V40Gy, but a slight difference for V30Gy, as shown in Table 5.

In the multivariate analysis, we observed a higher incidence of symptomatic RIRF in the group aged $\leq$ 77 years. This may be attributed to younger individuals potentially being more capable of expressing their pain. In the present study, 35.1 % of patients with fractures were symptomatic, in contrast to the previously reported value of 61 % post-radiotherapy for cervical cancer [21]. Treatments for cervical cancer are typically administered at younger ages than lung SBRT, with a median age between 50 and 70 years [22–24]. In consideration of the higher percentage of symptomatic fractures post-radiotherapy in cervical cancer, which has a lower median age, the present results showing a higher incidence of symptomatic fractures in the group aged $\leq$ 77 years appear to be consistent with these findings.

There were several limitations that need to be addressed. The implemented protocol underwent modifications in December 2008, which resulted in an escalated dosage and the incorporation of various protocols in the examination. Furthermore, this was a retrospective study conducted at a single institution. Therefore, it is inherently subject to biases typical of these investigations. Therefore, more extensive, multicenter studies are warranted to confirm the present results.

Conclusion

We herein investigated the relationships between the risk of RIRF and clinical and dosimetric factors following SBRT for early-stage NSCLC and examined differences in dosimetric parameters associated with symptomatic and asymptomatic RIRF. Among the 244 patients analyzed with a median follow-up period of 48 months, the 4-year cumulative incidence of grade $\geq$ 1 and grade $\geq$ 2 RIRF were 26.4 and 8.0 %, respectively. The median times to the onset of grade $\geq$ 1 and grade $\geq$ 2 RIRF were 20 and 18 months, respectively. Regarding clinical factors, a young age was associated with the development of grade $\geq$ 2 RIRF. The present results indicate that V40Gy $\leq$ 3.83 cc is the most effective indicator for the prevention of grade $\geq$ 2 RIRF among dose parameters in SBRT for early-stage NSCLC. The 4-year incidence of grade $\geq$ 2 RIRF with and without this threshold were 1.8 and 14.2 %, respectively.

Funding

This study was supported by a Grant-in-Aid for Research in Nagoya City University Number 2313003.

Role of the funding source

The funding institutions had no role in the design or conduct of the study.

CRediT authorship contribution statement

Nozomi Kita: Visualization, Writing – original draft, Formal analysis, Data curation, Conceptualization, Methodology. **Natsuo Tomita:** Funding acquisition, Conceptualization, Methodology, Writing – review & editing. **Taiki Takaoka:** Data curation. **Akane Matsuura:** Data curation. **Dai Okazaki:** Data curation. **Masanari Niwa:** Data curation. **Akira Torii:** Data curation. **Seiya Takano:** Data curation. **Yuji Mekata:** Data curation. **Akio Niimi:** Writing – review & editing. **Akio Hiwatashi:** Supervision, Writing – review & editing.

Declaration of Competing Interest

The authors declare that they have no known competing financial interests or personal relationships that could have appeared to influence the work reported in this paper.

References

[1] Chang JY, Senan S, Paul MA, Mehran RJ, Louie AV, Balter P, et al. Stereotactic ablative radiotherapy versus lobectomy for operable stage I non-small-cell lung cancer: a pooled analysis of two randomised trials. Lancet Oncol 2015;16(6):630–7.

[2] Tomita N, Okuda K, Kita N, Niwa M, Hashimoto S, Murai T, et al. Role of stereotactic body radiotherapy for early-stage non-small-cell lung cancer in patients borderline for surgery due to impaired pulmonary function. Asia Pac. J Clin Oncol 2022;18(6):634–41.

[3] Sogono P, Bressel M, David S, Shaw M, Chander S, Chu J, et al. Safety, Efficacy, and Patterns of Failure After Single-Fraction Stereotactic Body Radiation Therapy (SBRT) for Oligometastases. Int J Radiat Oncol Biol Phys 2021;109(3):756–63.

[4] Tomita N, Okuda K, Osaga S, Miyakawa A, Nakanishi R, Shibamoto Y. Surgery versus stereotactic body radiotherapy for clinical stage I non-small-cell lung cancer: propensity score-matching analysis including the ratio of ground glass nodules. Clin Transl Oncol 2021;23:638–47. https://doi.org/10.1007/S12094-020-02459-8.

[5] Pasalic D, Lu Yi, Betancourt-Cuellar SL, Taku N, Mesko SM, Bagley AF, et al. Stereotactic ablative radiation therapy for pulmonary metastases: Improving overall survival and identifying subgroups at high risk of local failure. Radiother Oncol 2020;145:178–85.

[6] Juan-Cruz C, Stam B, Belderbos J, Sonke JJ. Delivered dose-effect analysis of radiation induced rib fractures after thoracic SBRT. Radiother Oncol 2021;162:18–25. https://doi.org/10.1016/J.RADONC.2021.06.028.

[7] Asai K, Shioyama Y, Nakamura K, Sasaki T, Ohga S, Nonoshita T, et al. Radiation-induced rib fractures after hypofractionated stereotactic body radiation therapy: risk factors and dose-volume relationship. Int J Radiat Oncol Biol Phys 2012;84(3):768–73.

[8] Taremi M, Hope A, Lindsay P, Dahele M, Fung S, Purdie TG, et al. Predictors of radiotherapy induced bone injury (RIBI) after stereotactic lung radiotherapy. Radiat Oncol 2012;7(1). https://doi.org/10.1186/1748-717X-7-159.

[9] Mutter RW, Liu F, Abreu A, Yorke E, Jackson A, Rosenzweig KE. Dose-volume parameters predict for the development of chest wall pain after stereotactic body radiation for lung cancer. Int J Radiat Oncol Biol Phys 2012;82:1783–90. https://doi.org/10.1016/J.IJROBP.2011.03.053.

[10] Baba F, Shibamoto Y, Ogino H, Murata R, Sugie C, Iwata H, et al. Clinical outcomes of stereotactic body radiotherapy for stage I non-small cell lung cancer using different doses depending on tumor size. Radiat Oncol 2010;5(1). https://doi.org/10.1186/1748-717X-5-81.

[11] Kita N, Tomita N, Takaoka T, Sudo S, Tsuzuki Y, Okazaki D, et al. Comparison of Recurrence Patterns between Adenocarcinoma and Squamous Cell Carcinoma after Stereotactic Body Radiotherapy for Early-Stage Lung Cancer. Cancers (Basel) 2023;15. doi: 10.3390/CANCERS15030887.

[12] Kita N, Tomita N, Takaoka T, Okazaki D, Niwa M, Torii A, et al. Clinical and dosimetric factors for symptomatic radiation pneumonitis after stereotactic body radiotherapy for early-stage non-small cell lung cancer. Clin Transl Radiat Oncol 2023;41:100648.

[13] Shibamoto Y, Otsuka S, Iwata H, Sugie C, Ogino H, Tomita N. Radiobiological evaluation of the radiation dose as used in high-precision radiotherapy: Effect of prolonged delivery time and applicability of the linear-quadratic model. J Radiat Res 2012;53:1–9. https://doi.org/10.1269/jrr.11095.

[14] Baker S, Dahele M, Lagerwaard FJ, Senan S. A critical review of recent developments in radiotherapy for non-small cell lung cancer. Radiat Oncol 2016;11. https://doi.org/10.1186/S13014-016-0693-8.

[15] Kanda Y. Investigation of the freely available easy-to-use software "EZR" for medical statistics. Bone Marrow Transplant 2013;48:452–8. https://doi.org/10.1038/BMT.2012.244.
[16] Ma J-T, Liu Y, Sun Li, Milano MT, Zhang S-L, Huang L-T, et al. Chest Wall Toxicity After Stereotactic Body Radiation Therapy: A Pooled Analysis of 57 Studies. Int J Radiat Oncol Biol Phys 2019;103(4):843–50.
[17] Pettersson N, Nyman J, Johansson KA. Radiation-induced rib fractures after hypofractionated stereotactic body radiation therapy of non-small cell lung cancer: a dose- and volume-response analysis. Radiother Oncol 2009;91:360–8. https://doi.org/10.1016/J.RADONC.2009.03.022.
[18] Dunlap NE, Cai J, Biedermann GB, Yang W, Benedict SH, Sheng K, et al. Chest wall volume receiving >30 Gy predicts risk of severe pain and/or rib fracture after lung stereotactic body radiotherapy. Int J Radiat Oncol Biol Phys 2010;76:796–801. https://doi.org/10.1016/J.IJROBP.2009.02.027.
[19] Stephans KL, Djemil T, Tendulkar RD, Robinson CG, Reddy CA, Videtic GM. Prediction of chest wall toxicity from lung stereotactic body radiotherapy (SBRT). Int J Radiat Oncol Biol Phys 2012;82:974–80. https://doi.org/10.1016/J.IJROBP.2010.12.002.
[20] Welsh J, Thomas J, Shah D, Allen PK, Wei X, Mitchell K, et al. Obesity increases the risk of chest wall pain from thoracic stereotactic body radiation therapy. Int J Radiat Oncol Biol Phys 2011;81(1):91–6.
[21] Sapienza LG, Salcedo MP, Ning MS, Jhingran A, Klopp AH, Calsavara VF, et al. Pelvic Insufficiency Fractures After External Beam Radiation Therapy for Gynecologic Cancers: A Meta-analysis and Meta-regression of 3929 Patients. Int J Radiat Oncol Biol Phys 2020;106(3):475–84.
[22] Ogino I, Okamoto N, Ono Y, Kitamura T, Nakayama H. Pelvic insufficiency fractures in postmenopausal woman with advanced cervical cancer treated by radiotherapy. Radiother Oncol 2003;68:61–7. https://doi.org/10.1016/S0167-8140(03)00128-2.
[23] Mehmood Q, Beardwood M, Swindell R, Greenhalgh S, Wareham T, Barraclough L, et al. Insufficiency fractures in patients treated with pelvic radiotherapy and chemotherapy for uterine and cervical cancer. Eur J Cancer Care (engl) 2014;23(1):43–50.
[24] Schmeler KM, Jhingran A, Iyer RB, Sun CC, Eifel PJ, Soliman PT, et al. Pelvic fractures after radiotherapy for cervical cancer. Cancer 2010;116(3):625–30.